Journal of Applied Polymer Science

Morphological, thermal, and mechanical properties of poly(ε-caprolactone)/poly(ε-caprolactone)-grafted-cellulose nanocrystals mats produced by electrospinning

Caroline F. Bellani,[1,2] Eric Pollet,[2] Anne Hebraud,[2] Fabiano V. Pereira,[3] Guy Schlatter,[2] Luc Avérous,[2] Rosario E. S. Bretas,[1] Marcia C. Branciforti[4]

[1]Department of Materials Engineering, Federal University of Sao Carlos, Sao Carlos, Sao Paulo, Brazil
[2]ICPEES-ECPM, ICPEES UMR CNRS 7515, Université De Strasbourg, 25 Rue Becquerel, 67087 Strasbourg Cedex 2, France
[3]Department of Chemistry, Federal University of Minas Gerais, Belo Horizonte, Brazil
[4]Department of Materials Engineering, Engineering School of Sao Carlos, University of Sao Paulo, Sao Carlos, Sao Paulo, Brazil
Correspondence to: M. C. Branciforti (E-mail: marciacb@sc.usp.br)

ABSTRACT: Electrospun nanocomposites of poly(ε-caprolactone) (PCL) incorporated with PCL-grafted cellulose nanocrystals (PCL-*g*-CNC) were produced. PCL chains were grafted from cellulose nanocrystals (CNC) surface by ring-opening polymerization. Grafting was confirmed by infrared spectroscopy (FTIR) and thermogravimetric analyses (TGA). The resulting PCL-*g*-CNC were then incorporated into a PCL matrix at various loadings. Homogeneous nanofibers with average diameter decreasing with the addition of PCL-*g*-CNC were observed by scanning electron microscopy (SEM). PCL-*g*-CNC domains incorporated into the PCL matrix were visualized by transmission electron microscopy (TEM). Thermal and mechanical properties of the mats were analyzed by differential scanning calorimetry (DSC), TGA and dynamic mechanical analysis (DMA). The addition of PCL-*g*-CNC into the PCL matrix caused changes in the thermal behavior and crystallinity of the electrospun fibers. Significant improvements in Young's modulus and in strain at break with increasing PCL-*g*-CNC loadings were found. These results highlighted the great potential of cellulose nanocrystals as a reinforcement phase in electrospun PCL mats, which can be used as biomedical materials. © 2016 Wiley Periodicals, Inc. J. Appl. Polym. Sci. **2016**, *133*, 43445.

KEYWORDS: cellulose and other wood products; electrospinning; grafting; nanoparticles; nanowires; nanocrystals; polyesters

Received 23 April 2015; accepted 4 January 2016
DOI: 10.1002/app.43445

INTRODUCTION

The use of biomaterials has attracted special interest and played an important role in biomedical applications, as tissue engineering,[1] an interdisciplinary and multidisciplinary research field involving the use of living cells cultivated into polymeric scaffolds for development of functional substitutes for damaged tissue or organs.[2,3] A key goal of this area is to develop scaffolds with similar properties to those of extracellular matrices (ECMs) in order to help the tissue construction.[2,4]

Tissue engineering scaffolds, as ECM, should contain nanophase elements in order to mimic the nano/microsized scale of fibrous proteins.[5] Electrospinning is regarded as a simple and versatile top-down approach for the fabrication of uniform submicrometric fibers with long length scales in a continuous process.[6,7] Electrospun matrices are able to support the attachment and proliferation of a wide variety of cell types.[5] A broad range of materials such as synthetic and renewable polymers including collagens, chitosan, hyaluronic acid, poly(lactic acid), poly(glycolic acid), and poly(ε-caprolactone) (PCL) has been used for this purpose.[6,8,9]

PCL-based materials have emerged as a class of biomaterials of growing interest for applications in surgery as sutures, devices for bone fracture internal fixation, drug delivery and scaffolds for the regeneration of tissues or organs.[10,11] However, few issues need to be overcome to enlarge the use of PCL, as its limited mechanical strength which can be too low to ensure scaffold structural integrity for specific applications,[7,12–14] such as bone tissue engineering.[15–17] Therefore, enhancing mechanical properties of PCL-based scaffolds is desirable for biomedical applications, because the materials have to meet controllable mechanical requirements for handling implants and supporting the process of tissue regeneration and structure degradation.[7,8]

Cellulose nanocrystals (CNC) are short particles with high crystallinity in a length of micro to nanometers scale with an

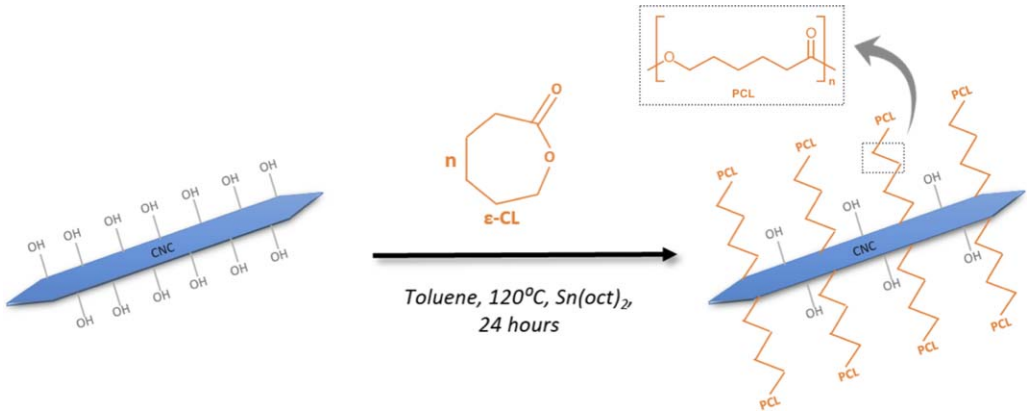

Scheme 1. Ring-opening polymerization of ε-caprolactone from the CNC surface. [Color figure can be viewed in the online issue, which is available at wileyonlinelibrary.com.]

estimated Young's modulus of 138 GPa and strength in the order of 7 GPa.[18,19] Excellent chemical and thermomechanical properties of CNC/polymer nanocomposites have been reported.[20–22] Nevertheless, the most significant inconvenience to the use of CNC in tissue engineering is their nondegradability, at best, slows degradability, by human body due to the lack of adequate cellulose enzymes (cellulases). However, researchers demonstrated that the degree of degradability can be influenced by the crystallinity of cellulose, and can be enlarged through oxidation steps.[23] Moreover, CNC are not expensive, simple to produce, largely available and, most importantly, biocompatible and more biodegradable,[24–27] making them suitable candidates as nano-reinforcements in biomaterials.

The main drawback to the use of cellulose nanocrystals for polymer nanocomposites is their inherent difficulty to disperse in nonpolar medium, because of their polar surface.[28] Hence, the nanocrystal-matrix interface is usually the weakest point in nanocomposites, which limits the global performance of the corresponding composite due to the fiber pull-out, rather than nanofiber break.[13] To overcome such effect and increase the compatibility with the polymeric matrix, chemical treatments must be performed on the cellulose surface, using different techniques and molecules.[20,22,29–33]

In the 'grafting from' method, the polymer chains are formed by in situ surface initiate polymerization.[29] This method enhances the interfacial adhesion between matrix and filler, which contributes to improve the mechanical properties of the final composite.[30] Zoppe *et al.*[13] previously studied the chemical grafting of low-molecular weight PCL 'onto' CNC and the addition of PCL-grafted CNC in PCL nonwoven mats. They reported the addition of PCL-grafted CNC induced the formation of annealed structures and heterogenous morphology along the nonwoven webs, decreasing the mechanical properties of the final nanocomposites. They attribute these results to the different rheological behavior of the PCL matrix (high-molecular weight) and the PCL-grafted chains (low molecular weight). Thus, the molecular weight of the PCL matrix must be considered when fabricating PCL nanofiber mats reinforced with PCL-grafted CNC. In the work of Sheng *et al.*,[14] unmodified CNC was used to reinforcing electrospun PCL mats. They showed the mechanical properties and thermal stability of the PCL/CNC nanocomposite fiber mats were improved. Hence, due to the CNC unique features as nano-reinforcement, with potential to tune the mechanical properties of scaffolds for tissue engineering, further studies must be achieved.

Previous studies have either used unmodified CNC[14] or CNC modified with PCL chains by grafting onto approaches.[13] In this study, PCL chains were grafted by ring-opening polymerization (ROP) 'from' the surfaces of CNC, which were obtained from eucalyptus wood by acid hydrolysis, in an effort to improve their compatibility with the PCL continuous phase. Afterwards, nanocomposites of PCL-grafted CNC incorporated into PCL were produced by electrospinning aiming to improve the mechanical properties of electrospun PCL mats. Finally, the morphology, the thermal and mechanical properties of the electrospun nanocomposites were characterized. The produced electrospun mats have potential uses in biomaterial application as drug delivery, substitute implants, tissue repair, and also as medium for cells culture because of the morphology, high porosity and biological properties of their constituents.

EXPERIMENTAL

Materials

Cellulose nanocrystals (CNC) were extracted from eucalyptus wood in the laboratories of the Federal University of Minas Gerais, Brazil, according to a previously described procedure based on acid hydrolysis by aqueous solution of sulfuric acid,[34] yielding CNC typically 160 nm long and 5 nm thick. The ε-caprolactone monomer (99%) was purchased from Acros Organics© and was dried 48 h over calcium hydride, distilled under reduced pressure and stored under nitrogen atmosphere prior to use. PCL ($M_n = 57$ kg/mol, PD = 1.8, determined by size-exclusion chromatography in chloroform with polystyrene standards) was provided by Perstorp© (commercial name CAPA™ 6806). Toluene RE (99.5%), n-heptane RE (99%) and *N, N*-dimethylformamide (DMF) RE (99.9%) were purchased from Carlo Erba©. Anhydrous toluene is obtained by refluxing over sodium and distillation. Dichloromethane (DCM) RE (99.8%), tin(II) ethyl hexanoate ($Sn(Oct)_2$) catalyst, and uranyl

acetate dihydrate (98%) were purchased from Sigma Aldrich and were used as received, without further purification.

ε-Caprolactone Ring Opening Polymerization from Cellulose Nanocrystals

Cellulose nanocrystals (CNC) were grafted with PCL chains by ROP, in a procedure adapted from the work of Habibi *et al.*[29] and sketched in Scheme 1. Lyophilized CNC (1 g) were placed in a three-neck flask, maintained under argon atmosphere. An amount of 50 ml of anhydrous toluene was added into the flask directly on the CNC. To improve dispersion, the suspension of CNC in toluene was maintained in a sonication bath for 5 min. Then, an azeotropic distillation of toluene was carried out to remove residual water. After this distillation, the required volume of anhydrous toluene (50 mL), previously distillated ε-caprolactone monomer (8 mL, with density of 1.03 g/mL) and tin(II) ethyl hexanoate [$Sn(Oct)_2$] (200 μL) were added into the flask. The polymerization proceeded for 24 h under magnetic stirring at 120 °C, and a few drops of aqueous HCl (1*M*) were added to stop the reaction. The modified CNC were recovered by precipitation in heptane and then filtered. In order to remove any nongrafted PCL chains (free PCL), the resulting PCL-grafted CNC were purified by Soxhlet extraction with toluene for 24 h and then with dichloromethane (DCM) for 24 h.

Fabrication of Electrospun Nanofiber Mats

Preparation of the Electrospinning Solutions. The electrospinning solutions were prepared with final PCL concentration of 19% w/w (considering the amount of PCL-grafted CNC) in 60/40 v/v DCM/DMF solvents mixture. Desired quantities of PCL-grafted CNC were dispersed at loadings of 1, 3 and 5 wt % of CNC in PCL. All solutions were sonicated for 5 min prior to electrospinning.

Electrospinning

Electrospun nanofibrous scaffolds of neat PCL, and PCL reinforced with PCL-grafted CNC were produced at room temperature and 80% humidity. A voltage of 30kV has been applied through a positive electrode connected to the tip of a needle (15 kV) plugged to a plastic syringe and syringe pump, and a negative electrode (−15 kV) attached to a grounded static collector plate covered with aluminum foil. All mats were electrospun for 20 min at a flow rate of 1.2 mL/h and a tip-to-collector distance of 15 cm.

Characterization

Infrared Spectroscopy (FTIR). Unmodified CNC, PCL-grafted CNC and neat PCL samples were characterized using a PerkinElmer infrared spectrometer model Spectrum 1000. The spectra were taken in the range $4000 - 750$ cm^{-1} using 32 scans and a scanning resolution of 4 cm^{-1}. The samples were previously dried for 24 h at 30 °C in a vacuum oven.

Scanning Electron Microscopy (SEM). The morphology of the nanofiber mats was observed in a Philips model XL30 scanning electron microscope, operating at 20 kV. Prior to observation, parts of all electrospun nanomats, collected on aluminum foil, were glued on a stub using a double-face carbon adhesive and gold-sputtered. Average diameter of the nanofibers (D) was measured using the Image-Pro Plus 4.5 software. Approximately 50 measurements per sample were performed to calculate the average values.

Transmission Electron Microscopy (TEM). Drops of aqueous dispersions of unmodified CNC and PCL-grafted CNC (0.01% w/v) were deposited on carbon-coated grid for electron microscope. Thin pieces of electrospun nanofibers were placed directly on copper grids. These samples were stained with uranyl acetate solution (2 wt %) during 2 min, and then allowed to dry. The samples were observed in a FEI Magellan model 400L, with acceleration voltage of 30 kV.

Dynamic Mechanical Analysis (DMA). The mechanical properties of the nanofiber mats were characterized using a dynamic-mechanical analyzer (DMA) model 8000 from Perkin-Elmer, in the controlled force mode, with a preload of 0.010 N and load rate of 0.5 N/min at room temperature. The glass transition temperature (T_g) of the nanocomposites was determined using constant frequency of 1 Hz, temperature range from −100 to 40 °C and heating ramp of 3 °C/min. The DMA samples were carefully peeled off from the surface of the aluminum foil and placed between weighting papers to avoid any damage. The sample dimensions were 10 mm in length, 8 mm in width and $0.10 - 0.15$ mm in thickness. Three samples were used to characterize each material.

Differential Scanning Calorimetry (DSC). The thermal properties of the electrospun mats were analyzed by differential scanning calorimetry (DSC), using DSC8000 equipment from Perkin-Elmer, under a nitrogen flow of 20 mL/min. The mat samples were first heated from −70 °C to 100 °C, maintained at 100 °C for 3 min and then cooled down to room temperature using a rate of 10 °C/min. From the heat of fusion (ΔH_m), the degree of crystallinity (X_c) of the samples was determined by using eq. (1):

$$Xc = \Delta H_m / w \ (\Delta H_m{}^o 100\%) * 100 \quad (1)$$

where w is weight fraction of the polymeric matrix in the nanocomposite (without CNC) and $\Delta H_m{}^o 100\%$ is the heat of fusion of a 100% crystalline PCL, 139.4 J/g.[35]

Thermogravimetric Analysis (TGA). The thermal stability of the samples was analyzed by thermogravimetric analyses (TGA) using a Perkin-Elmer thermoanalyser model Pyris 1. Thermograms were recorded from room temperature to 600 or 700 °C at a heating rate of 10 °C/min under nitrogen flow of 20 mL/min. The unburnt residue left at 650 °C was used to calculate the CNC content in PCL-grafted CNC. Since the neat CNC shows 18% residue and neat PCL has no residue, the CNC content in the grafted cellulose nanocrystals can be calculated by dividing the experimental residue recorded for the PCL-grafted CNC (expressed in %) by 18.

RESULTS AND DISCUSSION

The thermogravimetric analysis under nitrogen of the unmodified cellulose nanocrystals (CNC), Figure1(a), indicated first a mass loss of 6% probably due the water and volatile products between $30 - 100$ °C. A second mass loss with an onset degradation temperature of 260 °C and a maximum degradation temperature at approximately 314 °C typical of cellulose

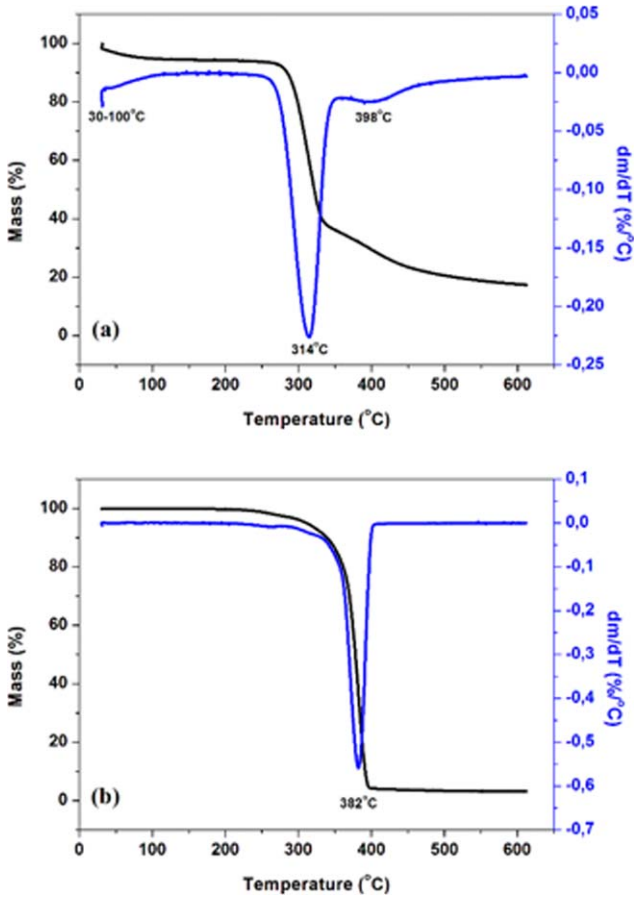

Figure 1. TGA thermograms of (a) cellulose nanocrystals (CNC) and (b) PCL-grafted CNC. [Color figure can be viewed in the online issue, which is available at wileyonlinelibrary.com.]

nanocrystals[36] was observed. A third degradation peak, with a maximum at 398 °C and a mass loss of about 10% was also observed. The residue at 650 °C of the CNC was about 18%. These last two results are related to the hydrolysis time with sulfuric acid during the extraction process of the CNC. Regions of CNC which do not bind to sulfate groups have greater thermal stability. The sulfate groups on the CNC surface tend to promote the CNC thermal degradation and remain as residue after the thermal analysis under nitrogen.[37,38] On the other hand, the thermogravimetric analysis of the grafted cellulose nanocrystals (PCL-grafted CNC), Figure 1(b), displayed an onset degradation temperature around 295 °C and a maximum degradation temperature at 382 °C, consistent with the temperature range for lower molar mass due to PCL degradation.[39] The residue at 650 °C was about 2%. As described above, the CNC has an 18% residue; and on the premise that the thermodegradation of PCL has no residue, the CNC content in the grafted cellulose nanocrystals could be calculated. This content was found to be between 10 and 12%.This result shows the grafting process was effective.

The PCL grafting process from cellulose nanocrystals was also confirmed by FTIR analyses. The FTIR spectra of the unmodified cellulose nanocrystals (CNC), PCL-grafted CNC nanocrystals and neat PCL are shown in Figure 2. In comparison with the pure cellulose nanocrystals spectra, the PCL-grafted CNC spectrum shows, even after Soxhlet extraction, the presence of the band at 1730cm^{-1}, characteristic of the axial deformation of the carbonyl (C═O) group from PCL. Moreover, a lower band intensity of the axial deformation of the OH bonds at 3330 cm^{-1} was also observed, suggesting the effective grafting of PCL at the surface of the CNC. These results are in accordance with the patterns of FTIR spectra previously obtained by Habibi *et al.*[29]

Figure 3 shows SEM images obtained for the electrospun mats of (a) neat PCL, (b) PCL with 1 wt %, (c) with 3 wt %, and (d) with 5 wt % of PCL-grafted CNC. The global appearance and morphology of the corresponding mats were preserved, even after the addition of PCL-grafted CNC. However, it can be observed that the average fiber diameter (D) decreases when adding the PCL-grafted CNC (Figure 3 and Table I). Indeed, in the present work, the diameter of the nanofibers produced under the same conditions decreased from 640 nm for the neat PCL to 180 nm for the PCL + 1 wt % PCL-*g*-CNC fibers and 165 nm for the PCL + 2 wt % and 5 wt % PCL-*g*-CNC fibers. This diameter reduction can be probably attributed to the addition of the PCL-*g*-CNC leading to an increase of the electrospinning solution conductivity. This observation clearly corroborates the previous works of Shi *et al.*[19] and Xiang *et al.*,[22] which have studied the morphology of electrospun nanofibers of poly(lactic acid) reinforced with cellulose nanocrystals. The authors observed an increase in the electrical conductivity of the solution due to the presence of sulfate ester groups on the CNC surface, resulting in a higher charge density on the surface of ejected jet, which promote the formation of higher elongation forces and thus, producing fibers with smaller diameter.

In order to analyze the effect of the incorporation of PCL-grafted CNC into the PCL matrix, the corresponding mats were observed by TEM. In Figure 4, micrographs of (a) neat PCL nanofibers, (b) PCL + 1 wt %, (c) PCL + 3 wt % and (d)

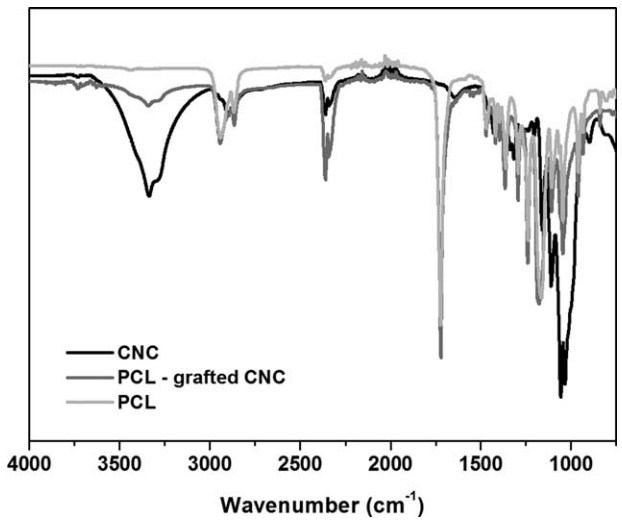

Figure 2. FTIR spectrum of cellulose nanocrystals (CNC), PCL-grafted CNC, and neat PCL.

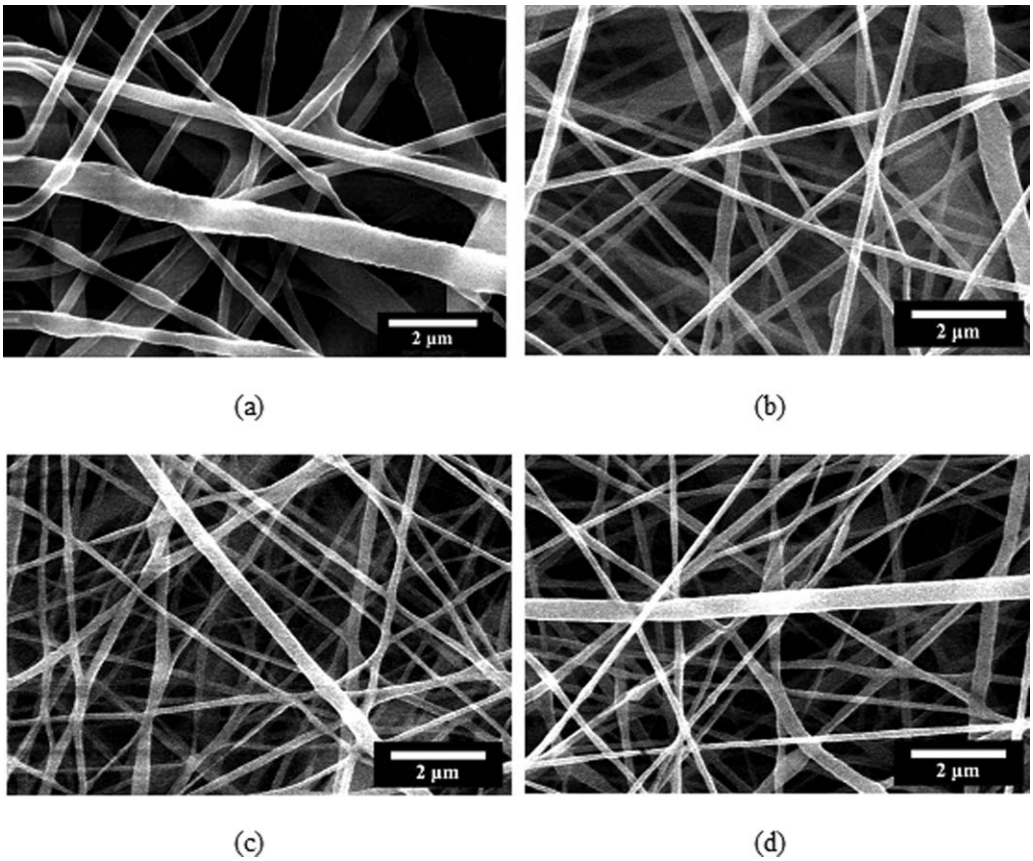

Figure 3. SEM images of electrospun mats of (a) neat PCL, and PCL with (b) 1 wt % (c) 3 wt %, and (d) 5 wt % PCL-grafted CNC.

PCL + 5 wt % of PCL-grafted CNC are shown. The slightly dark regions observed in Figure 4(a) are due to PCL fibers overlapping. In Figure 4(b–d), the PCL-grafted CNC domains are visualized as denser lines (dark) indicated by arrows, while the less dense areas (brighter) represent the PCL domains. The PCL-grafted CNC domains show a thin and aligned shape with good distribution within PCL fibers. The TEM analysis showed the PCL-grafted CNC were incorporated into the PCL matrix, and the corresponding nanocomposites were successfully obtained while preserving the global appearance and general morphology of nanofiber mats, as previously shown by the SEM analysis (Figure 3).

DSC experiments were performed on the fibrous mats in the temperature range of −70 °C to 100 °C. In this temperature range, no specific degradation of the PCL-*g*-CNC can occur as previously shown by TGA analysis. From the first heating curves, Figure 5(a), the melting temperature (Tm) and the degree of crystallinity (X_c) of the sample were obtained (Table I). There was an increase in Tm with the PCL-grafted CNC addition, indicating the production of more perfect crystallites. The degree of crystallinity of the samples also increased with the PCL-grafted CNC addition. Such a result was also observed by Habibi *et al.*[29] with PCL casting films and unmodified or modified (PCL-grafted) cellulose nanocrystals. They noted the grafting procedure contributes considerably to increase the degree of crystallinity of the corresponding bionanocomposite. The crystallization temperature of the samples (T_c) was obtained from the cooling curve, Figure 5(b), after erasing the previous thermal history. An increase in the Tc of the nanocomposites with an increase in the amount of PCL-grafted CNC was observed, which means the filler surface probably acts as nucleation sites for the PCL chains crystallization under quiescent conditions. The main relaxation temperature which can be associated with glass transition temperature (T_g) of the nanocomposites, determined from DMA curves, not shown here, was not affected by the incorporation of PCL-

Table I. Average Fibers Diameter (D), Thermal Properties and Degree of Crystallinity (X_c) of the Samples

Sample	D (nm)	T_m (°C)	ΔH_m (Jg^{-1})	T_c (°C)	X_c (%)	T_g (°C)
PCL	636.9 ± 62.1	60.0 ± 2.1	80.9 ± 0.1	41.3 ± 1.4	58.0 ± 0.1	−60.0 ± 1.5
PCL + 1wt % PCL-*g*-CNC	182.1 ± 11.9	62.8 ± 1.8	81.7 ± 0.1	41.4 ± 1.8	59.2 ± 0.1	−60.5 ± 2.2
PCL + 3wt % PCL-*g*- CNC	164.7 ± 8.9	66.2 ± 2.3	82.5 ± 0.2	44.3 ± 1.4	61.0 ± 0.2	−60.8 ± 2.5
PCL + 5wt % PCL-*g*- CNC	166.4 ± 7.5	67.8 ± 1.5	84.4 ± 0.2	46.7 ± 2.0	63.2 ± 0.2	−61.3 ± 1.8

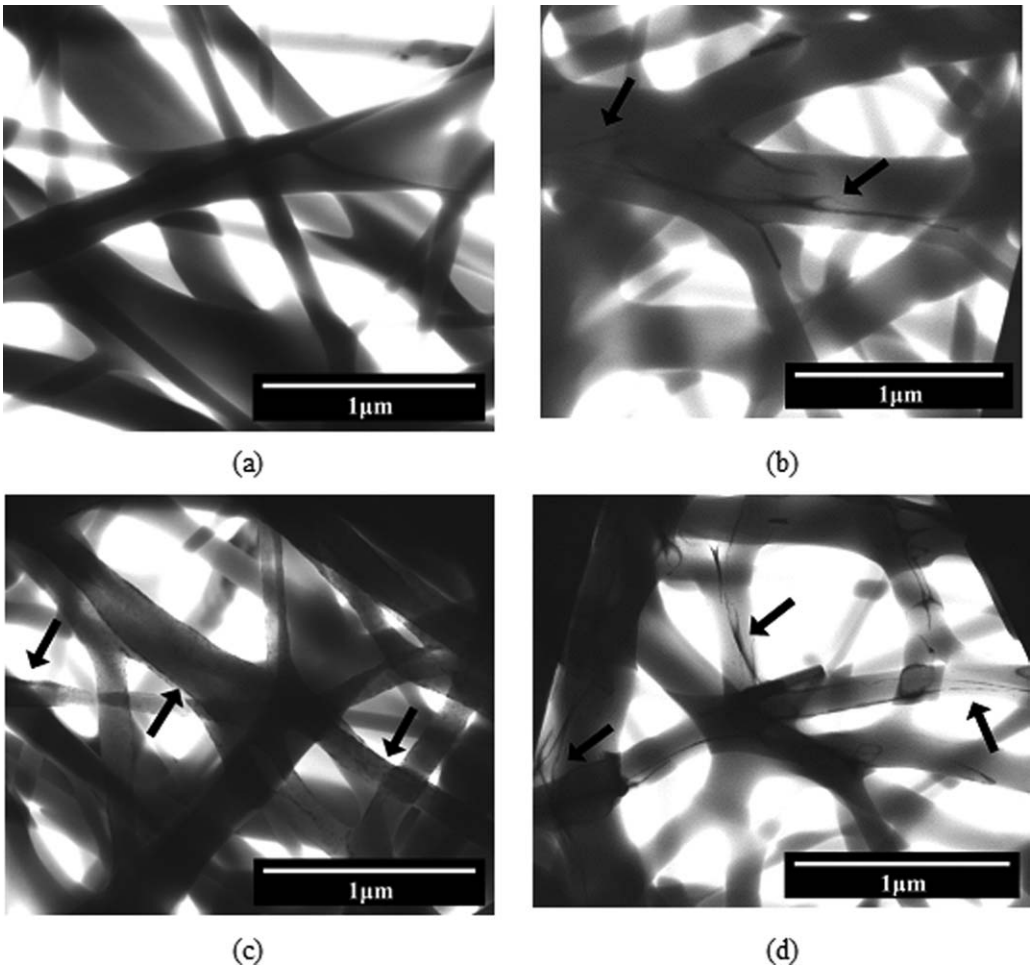

Figure 4. TEM images of electrospun mats of (a) neat PCL, and PCL with (b) 1 wt % (c) 3 wt %, and (d) 5 wt % PCL-grafted CNC. Arrows are pointing to some PCL-grafted CNC domains.

grafted CNC (Table I), indicating the CNC did not interfere with the relaxation of the PCL amorphous phase.

Figure 6 shows the results of the thermogravimetric analyses for the electrospun mats formed of neat PCL and PCL with 1 wt %, 3 wt %, and 5 wt % of PCL-grafted CNC. These results clearly indicate a decrease in the thermal stability of the PCL mats with increasing content of PCL-grafted CNC in the bionanocomposites, as expected due to the lower thermal stability of the PCL-grafted CNC as already described. The neat PCL mat shows a maximum degradation temperature at ~450 °C and no residue. As showed above (Figure 1), the PCL-grafted CNC shows a maximum degradation temperature around 380 °C. The lower temperature observed for the PCL-grafted CNC is likely due to shorter chains (lower molar masses) of the PCL grafts compared to the commercial PCL matrix (with M_n of 57 kg/mol). The neat PCL mat has a maximum degradation temperature of approximately 50 °C higher than the bionanocomposites with 3 wt % and 5 wt % of PCL-*g*-CNC. Therefore, the thermal degradation of the two components in the bionanocomposites is not independent; as the PCL-*g*-CNC thermal degradation occurs first, thus the thermal degradation of the PCL matrix tends to occur at lower temperature. In addition, one cannot exclude that the residual sulfate groups from CNC negatively affect the bionanocomposites thermal stability.

As shown in Figure 7, the Young's modulus (E) and the tension at break (σ_b) of the PCL nanomats increased when the PCL-grafted CNC was added, indicating that stiffer and more performing nanomats were obtained. The addition of 5 wt % of PCL-grafted CNC increased the elastic modulus by over 50%. However, with increased PCL-grafted CNC content, the elongation at break (ε_b) of the bionanocomposite mats decreased. These results indicated a good dispersion and interface between the PCL-grafted CNC and the PCL matrix was developed. The spread in the data is fairly typical reflecting variations in the randomly deposited electrospun mats.

Mechanical properties of nonwoven electrospun mats are influenced by several factors related to processing and solution conditions. Thomas *et al.*[40] studied the mechanical and morphological properties of PCL electrospun mats fabricated at different collector rotation speeds. They observed that the mechanical properties (modulus and tensile strength) of the mats increased gradually with increasing collector rotation speed. This behavior was attributed to the increased fiber alignment and packing and the decrease in interfiber pore size at

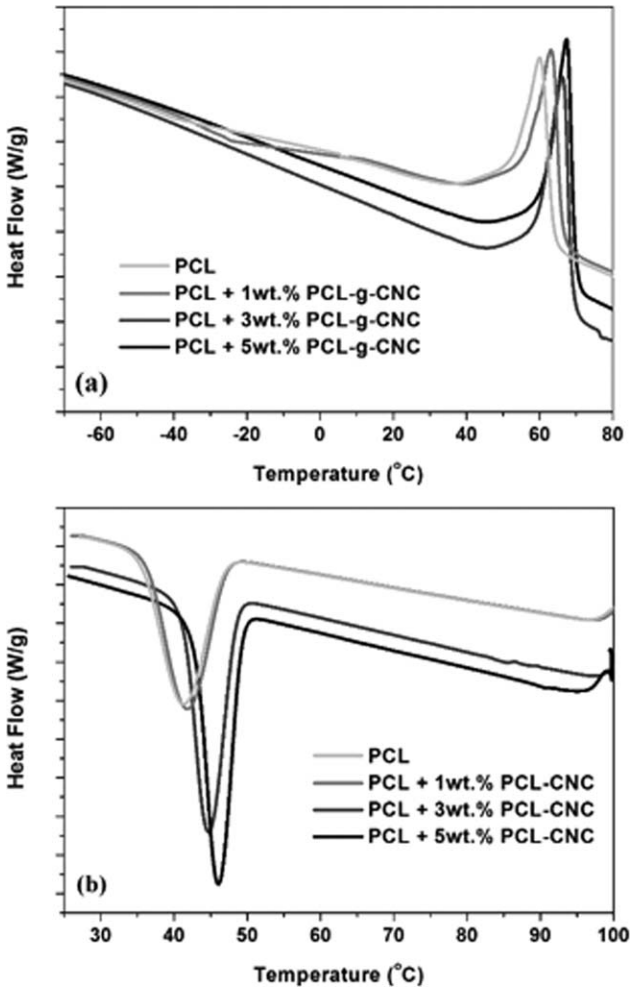

Figure 5. DSC (a) heating and (b) cooling thermograms of neat PCL, and PCL with 1 wt %, 3 wt %, and 5 wt % PCL-grafted CNC electrospun mats.

higher collector rotating speeds. In our case, a static collector was used. Zoppe *et al.*[13] have demonstrated that the mechanical behavior of nanocomposites formed of PCL incorporated with

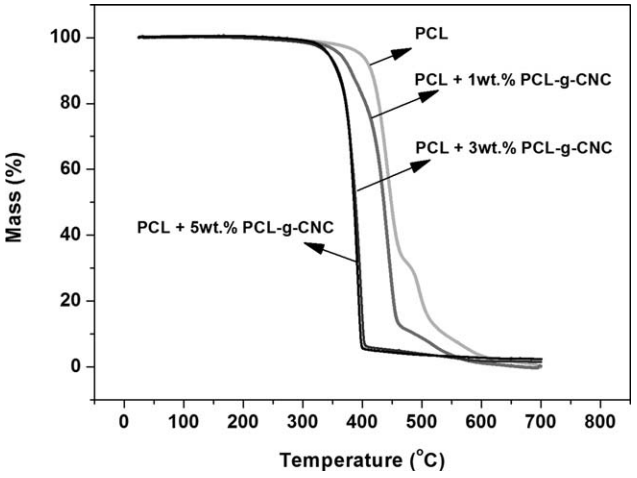

Figure 6. TGA thermograms of neat PCL, and PCL with 1 wt %, 3 wt %, and 5 wt % PCL-grafted CNC electrospun mats.

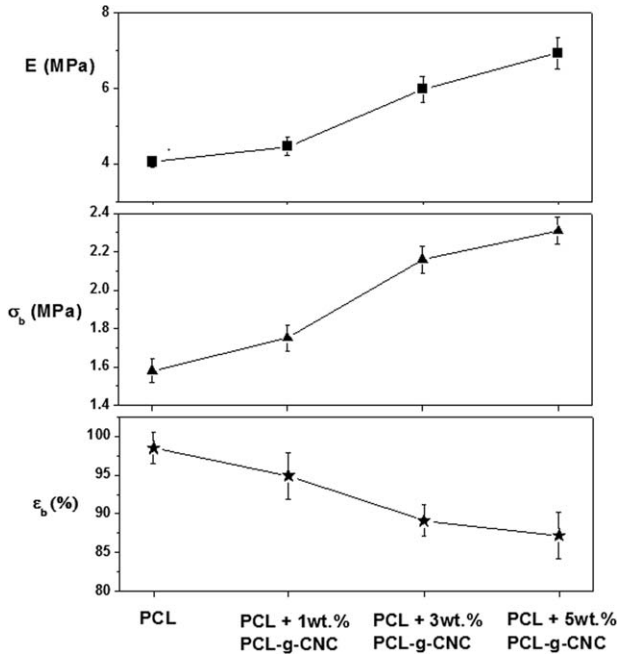

Figure 7. Elastic modulus (E), tensile at break (σ_b), and elongation at break (ε_b) of the electrospun mats samples.

unmodified and modified (PCL-grafted) cellulose nanocrystals are intimately related to the reinforcing effect of the CNC filler and also to the nanofiber diameter. The density of entanglements and its distribution are better in fibers with smaller diameters due to the higher surface area. In the work of Lönnberg *et al.*[32] the highest mechanical properties of PCL bionanocomposite reinforced with grafted microfibrillated cellulose (MFC) were obtained for the longest PCL graft length and with a high loading in MFC (10 wt %).

Therefore, according to our results, the incorporation of PCL-grafted CNC, even in small amounts, increased considerably the mechanical properties of PCL nanofiber mats. The improvements in mechanical behavior can be attributed to the addition of PCL-grafted CNC to the fiber, and probably to the higher molecular weight (longer chains) of the grafted PCL chains, and to respective decrease in the fibers diameter. Thus, from these analyses, it is clear the grafting procedure contributed to rise (even slightly) the degree of crystallinity and to considerably increase the mechanical strength and stiffness of the bionanocomposites.

CONCLUSIONS

The grafting of PCL chains from cellulose nanocrystals was successfully obtained via *in situ* ring opening polymerization reaction; the resulting poly(ε-caprolactone)-grafted cellulose nanocrystals with PCL chains displayed good thermal stability and has a CNC content of approximately 10-12%. Homogeneous electrospun mats of bionanocomposites formed of PCL with PCL-grafted CNC were produced; it was observed the average fiber diameter decreased with the addition of the PCL-grafted CNC. The grafted CNC was successfully dispersed into a PCL matrix. There was a significant increase in the melting

temperature and in the crystallization temperature of the electrospun PCL nanofibers with the addition of the grafted CNC. Also, an increase in the degree of crystallinity of the PCL mats with the addition of the grafted CNC indicated a good compatibility between the matrix and the filler occurred. The incorporation of the PCL-grafted CNC, even in small amounts, increased considerably the mechanical properties of the nanofiber mats, with significant improvements in the Young's modulus and the tension at break. Therefore, it becomes clear the potential use of cellulose nanocrystals as a reinforcement phase in electrospun PCL mats.

ACKNOWLEDGMENTS

Authors thank CAPES for the financial support (CAPES/Nanobiotec No13 and CAPES/COFECUB No670/10). The author MCB acknowledges the CNPq for the financial support (N°309779/2010-3).

REFERENCES

1. Tian, H.; Tang, Z.; Zhuang, X. *Prog. Polym. Sci.* **2012**, *37*, 237.
2. Burg, K. J. L.; Porter, S.; Kellam, J. F. *Biomaterials* **2000**, *21*, 2347.
3. Langer, R.; Vacanti, J. *Science* **1993**, *260*, 920.
4. Freed, L. E.; Vunjak-Novakovic, G.; Biron, R. J.; Eagles, D. B.; Lesnoy, D. C.; Barlow, S. K.; Langer, R. *Nat. Biotechnol.* **1994**, *12*, 689.
5. Sill, T. J.; von Recum, H. A. *Biomaterials* **2008**, *29*, 1989.
6. Sun, B.; Long, Y. Z.; Zhang, H. D.; Li, M. M.; Duvail, J. L.; Jiang, X. Y.; Yin, H. L. *Prog. Polym. Sci.* **2014**, *39*, 862.
7. Tamayol, A.; Akbari, M.; Annabi, N.; Paul, A.; Khademhosseini, A.; Juncker, D. *Biotechnol. Adv.* **2013**, *31*, 669.
8. Agarwal, S.; Wendorff, J. H.; Greiner, A. *Adv. Mater.* **2009**, *21*, 3343.
9. Wang, X.; Ding, B.; Li, B. *Mater. Today* **2013**, *16*, 229.
10. Kim, G. M.; Le, K.; Giannitelli, S.; Lee, Y.; Rainer, A.; Trombetta, M. *J. Mater. Sci. Mater. Med.* **2013**, *24*, 1425.
11. Ruckh, T. T.; Kumar, K.; Kipper, M. J.; Popat, K. C. *Acta Biomater.* **2010**, *6*, 2949.
12. Ghasemi-Mobarakeh, L.; Prabhakaran, M. P.; Morshed, M.; Nasr-Esfahani, M. H.; Ramakrishna, S. *Biomaterials* **2008**, *29*, 4532.
13. Zoppe, J. O.; Peresin, M. S.; Habibi, Y.; Venditti, R. A.; Rojas, O. J. *ACS Appl. Mater. Interfaces* **2009**, *1*, 1996.
14. Sheng, L.; Jiang, R.; Zhu, Y.; Ji, Y. *J. Macromol. Sci. Part B: Phys.* **2014**, *53*, 820.
15. Bose, S.; Roy, M.; Bandyopadhyay, A. *Trends Biotechnol.* **2012**, *30*, 546.
16. Diba, M.; Kharaziha, M.; Fathi, M. H.; Gholipourmalekabadi, M.; Samadikuchaksaraei, A. *Compos. Sci. Technol.* **2012**, *72*, 716.
17. Woodruff, M. A.; Hutmacher, D. W. *Prog. Polym. Sci.* **2010**, *35*, 1217.
18. Nishino, T.; Takano, K.; Nakamae, K. *J. Polym. Sci. Part B: Polym. Phys.* **1995**, *33*, 1647.
19. Shi, Q.; Zhou, C.; Yue, Y.; Guo, W.; Wu, Y.; Wu, Q. *Carbohydr. Polym.* **2012**, *90*, 301.
20. Rescignano, N.; Fortunati, E.; Montesano, S.; Emiliani, C.; Kenny, J. M.; Martino, S.; Armentano, I. *Carbohydr. Polym.* **2014**, *99*, 47.
21. Siqueira, G.; Brasa, J.; Follain, N.; Belbekhouche, S.; Marais, S.; Dufresne, A. *Carbohydr. Polym.* **2013**, *91*, 711.
22. Xiang, C.; Joo, Y. L.; Frey, M. W. *J. Biobased Mater. Bioenergy* **2009**, *3*, 147.
23. Lin, N.; Dufresne, A. *Eur. Polym. J.* **2014**, *59*, 302.
24. Jackson, J. K.; Letchford, K.; Wasserman, B. Z.; Ye, L.; Hamad, W. Y.; Burt, H. M. *Int. J. Nanomed.* **2011**, *6*, 321.
25. Lam, E.; Male, K. B.; Chong, J. H.; Leung, A. C. W.; Luong, J. H. T. *Trends Biotechnol.* **2012**, *30*, 283.
26. Mahmoud, K. A.; Mena, J. A.; Male, K. B.; Hrapovic, S.; Kamen, A.; Luong, J. H. T. *ACS Appl. Mater. Interfaces* **2010**, *2*, 2924.
27. Kümmerer, K.; Menz, J.; Schubert, T.; Thielemans, W. *Chemosphere* **2011**, *82*, 1387.
28. Oksman, K.; Mathew, A. P.; Bondeson, D.; Kvien, I. *Compos. Sci. Technol.* **2006**, *66*, 2776.
29. Habibi, Y.; Goffin, A. L.; Schiltz, N.; Duquesne, E.; Dubois, P.; Dufresne, A. *J. Mater. Chem.* **2008**, *18*, 5002.
30. Habibi, Y. *Chem. Soc. Rev.* **2014**, *43*, 1519.
31. Krouit, M.; Bras, J.; Belgacem, M. N. *Eur. Polym. J.* **2008**, *44*, 4074.
32. Lonnberg, H.; Larsson, K.; Lindstrom, T.; Hult, A.; Malmstro, E. *Appl. Mater. Interfaces* **2011**, *3*, 1426.
33. Morelli, C. L.; Belgacem, M. N.; Branciforti, M. C.; Bretas, R. E. S.; Crisci, A.; Bras, J. *Compos.: Part A* **2015**, doi: 10.1016/j.compositesa.2015.10.038.
34. Mesquita, J. P.; Patricio, P. S. O.; Donnici, C. L.; Petri, D. F. S.; Oliveira, L. C.; Pereira, F. V. *Soft Matter* **2011**, *7*, 4405.
35. Crescenzi, V.; Manzini, G.; Calzolari, G.; Borri, C. *Eur. Polym. J.* **1972**, *8*, 449.
36. Morelli, C. L.; Marconcini, J. M.; Pereira, F. V.; Bretas, R. E. S.; Branciforti, M. C. *Macromol. Symp.* **2012**, *319*, 191.
37. Roman, M.; Winter, W. T. *Biomacromolecules* **2004**, *5*, 1671.
38. Teodoro, K. B.; Teixeira, E. M.; Corrêa, A. C.; de Campos, A.; Marconcini, J. M.; Mattoso, L. H. *Polímeros* **2011**, *21*, 280.
39. Unger, M.; Vogel, C.; Seisler, H. *Appl. Spectroscopy* **2010**, *64*, 805.
40. Thomas, V.; Jose, M. V.; Chowdhury, S.; Sullivan, J. F.; Dean, D. R.; Vohra, Y. K. *J. Biomater. Sci. Polym. Ed.* **2006**, *17*, 969.